

## Ultranarrow Optical Absorption and Two-Phonon Excitation Spectroscopy of $\text{Cu}_2\text{O}$ Paraexcitons in a High Magnetic Field

Jan Brandt, Dietmar Fröhlich, Christian Sandfort, and Manfred Bayer  
*Institut für Physik, Universität Dortmund, D-44221 Dortmund, Germany*

Heinrich Stolz

*Fachbereich Physik, Universität Rostock, D-18501 Rostock, Germany*

Nobuko Naka

*Department of Applied Physics, The University of Tokyo, Tokyo 113-8656, Japan*

(Received 27 February 2007; revised manuscript received 27 June 2007; published 19 November 2007)

We show that in a magnetic field  $B$  the otherwise forbidden lowest exciton in  $\text{Cu}_2\text{O}$  (paraexciton of  $\Gamma_2^+$  symmetry) gives rise to a narrow absorption line of 80 neV at a temperature of 1.2 K. The  $B^2$  dependence of the field-induced oscillator strength and the low energy shift  $\Delta E$  with increasing field strength are measured. From two-phonon excitation spectroscopy measurements we derive by a merely kinematical analysis a very reliable value for the paraexciton mass. A blueshift and a broadening of the absorption line are observed for increasing excitation intensity. These observations are discussed in connection with a Bose-Einstein condensation of paraexcitons in  $\text{Cu}_2\text{O}$ .

DOI: [10.1103/PhysRevLett.99.217403](https://doi.org/10.1103/PhysRevLett.99.217403)

PACS numbers: 78.20.Ls, 71.35.Cc, 71.35.Lk, 71.36.+c

Very recently the intense activities to obtain an excitonic Bose-Einstein condensate (BEC) have been mostly focused on confined semiconductor heterostructures such as indirect excitons in coupled quantum wells [1] or polaritons in microcavities [2,3]. While showing very promising results, condensatelike phenomena in these systems are most likely obtained far from equilibrium due to rather short carrier lifetimes. Still the candidates which come closest to the requirements for a quasiequilibrium excitonic BEC are the lowest exciton transitions in  $\text{Cu}_2\text{O}$ . These excitons of the so-called yellow series consist of a three-fold orthoexciton of  $\Gamma_5^+$  symmetry, which is only quadrupole allowed and a paraexciton of  $\Gamma_2^+$  symmetry, which is optically forbidden. The orthoexciton is split off from the paraexciton by 12 meV to higher energy due to isotropic exchange. It was recently shown by high resolution spectroscopy that the orthoexciton can split in up to three components by anisotropic exchange [4].

In most experiments concerning BEC in  $\text{Cu}_2\text{O}$  nonresonant or resonant excitation of the orthoexcitons was studied [5–7]. The orthoexcitons decay on a nanosecond time scale to paraexcitons [8]. Because of the energy shift of 12 meV this scheme of paraexciton excitation leads to hot paraexcitons, which have to cool down by exciton-exciton and/or acoustic phonon interaction to exhibit at high densities BEC with a macroscopic population at  $k = 0$ .

Direct excitation by absorption at  $k = k_0$  (photon wave number) yields ultracold excitons. High resolution experiments in a magnetic field allow one to measure paraexciton absorption spectra as was first shown in Ref. [9]. At 10 T and 1.2 K we get in high quality samples an absorption coefficient of about  $80 \text{ cm}^{-1}$  with an extremely small linewidth of 80 neV. Because of the high resolution of

our absorption measurements we are able to measure directly a blueshift and an increase of linewidth which point to an onset of repulsive interaction, a necessary prerequisite for a phase transition of the exciton gas to a condensate. For a weakly interacting Bose gas of excitons, the critical density  $n_c$  depends only on the product of exciton mass  $M$  and critical temperature  $T_c$ . The exciton mass is therefore the decisive parameter to calculate a BEC phase diagram. As discussed in detail in Ref. [10], mass values between  $2.2m_0$  and  $2.7m_0$  are cited in the literature. These values are gained from different line shape analyses. Making again use of our high resolution laser setup, we are able to determine the exciton mass  $M_p$  by two-phonon excitation spectroscopy. The purely kinematical analysis requires only the sound velocity as an input parameter, which is known even at low temperatures. Our experimental technique yields in addition a value for the background refractive index  $n$  at the paraexciton resonance, which agrees well with an early publication [11] and recent measurements [12]. From our analysis we get  $M_p = (2.61 \pm 0.04)$  (in units of free electron mass  $m_0$ ) and  $n = 2.94 \pm 0.05$  and a kinetic energy  $E_0 = \hbar^2 n^2 k_0^2 / (2M_p m_0) = (13.2 \pm 0.2) \mu\text{eV}$ , which corresponds in thermal equilibrium to a temperature of 0.15 K.

In the following we will give a short description of our experimental setup and the theory of magnetic field-induced mixing of ortho- and paraexcitons. We will present our experimental results as function of field strength and intensity. After presentation of the two-phonon measurements we will give an analysis of the data and discuss their implications on BEC of paraexcitons in  $\text{Cu}_2\text{O}$ .

For our measurements we used a single frequency dye laser (Coherent 899-29) with a bandwidth of about 5 neV

[4,13]. A 10 Tesla magneto-optical cryostat allowing measurements in Faraday and Voigt configuration was used. Pumping on the variable temperature inset we achieved temperatures down to 1.2 K. For the two-phonon excitation spectroscopy we used the quadrupole emission of the paraexciton (outgoing resonance) to monitor the two-phonon (optical and longitudinal acoustical phonon) excitation processes as function of laser energy. The main advantage of this method lies in the fact that the accuracy of the energy reading of the phonon resonances depends only on the photon energy of the laser which is directly measured by a wave meter (High Finesse WS-U 30, accuracy of 100 neV). Measurements in forward and backward configuration lead to the same results. Strain-free preparation and mounting of the samples is of great importance to avoid inhomogeneities and thus to obtain narrow resonances.

As shown in detail in Ref. [14], the orthoexciton splits in a magnetic field into three components with quantum numbers  $M = 0$  and  $M = \pm 1$ . The paraexciton of  $\Gamma_2^+$  symmetry mixes with the  $M = 0$  component of the orthoexciton [15,16], thus gaining quadrupole oscillator strength. For the field-induced mixing coefficient  $a_O$  and the repulsion  $\Delta E$  of the  $M = 0$  orthoexciton and the paraexciton we get

$$a_O = \frac{\alpha_B B}{\sqrt{(\alpha_B B)^2 + \epsilon^2}} \approx \frac{\alpha_B B}{\epsilon} \quad \text{and} \quad \Delta E \approx \frac{(\alpha_B B)^2}{\epsilon} \quad (1)$$

with the parameters  $\epsilon = 12.12$  meV and  $\alpha_B = 92.5$   $\mu\text{eV}/\text{T}$  [14]. The paraexciton oscillator strength  $f_P$  is related to the orthoexciton oscillator strength  $f_O$  by:

$$f_P(B) = \left(\frac{\alpha_B B}{\epsilon}\right)^2 f_O = 5.8 \times 10^{-5} f_O B^2. \quad (2)$$

For 10 T the oscillator strength of the paraexciton is only 0.006 of the oscillator strength of the orthoexciton ( $\mathbf{B} \parallel \mathbf{k} \parallel [110]$  and polarization  $\mathbf{e} \parallel [001]$ ).

In Fig. 1 we present an absorption measurement of a 250  $\mu\text{m}$  sample in a field of  $B = 10$  T at a temperature of 1.2 K with a laser intensity of less than 0.5  $\text{W}/\text{cm}^2$ . The spectrum was taken in Faraday configuration ( $\mathbf{B} \parallel \mathbf{k} \parallel [110]$ ). According to the quadrupole selection rules the transition is allowed for a laser polarization  $\mathbf{e} \parallel [001]$ . The laser was scanned across the crystal for selection of highest absorption (80  $\text{cm}^{-1}$ ). Under these conditions the smallest linewidth was about 80 neV. There is an almost perfect fit to a Lorentzian (solid line) suggesting only a small inhomogeneous broadening. The magnetic field dependence of the absorption coefficient up to 10 T is shown in the right inset. The dashed line is a fit of the low field data to a  $B^2$  dependence. For each field setting the laser spot on the sample had to be readjusted for maximum absorption because of slight movements of the sample. The deviations at high field strength from the predicted  $B^2$  dependence [Eq. (2)] are probably caused by a reduced

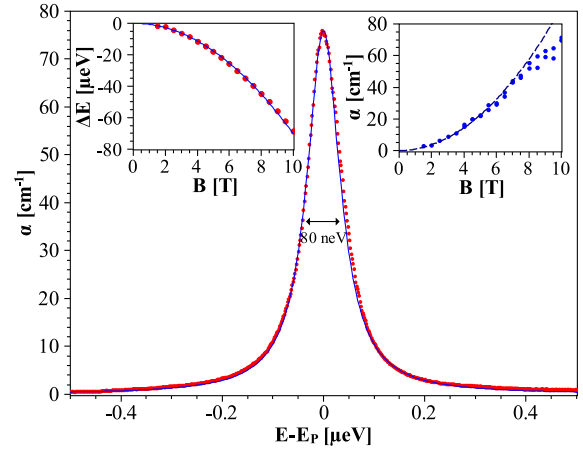


FIG. 1 (color online). Absorption coefficient  $\alpha(E)$  of paraexciton resonance in a magnetic field of 10 T at a temperature of 1.2 K;  $\mathbf{B} \parallel \mathbf{k}$  (Faraday configuration) with  $\mathbf{k} \parallel [110]$  and polarization  $\mathbf{e} \parallel [001]$ ; full dots, experimental results; solid line, fit to a Lorentzian with full width half maximum (FWHM) 80 neV, resonance energy  $E_P = 2.020598$  eV. Right inset:  $B$ -field dependence of absorption coefficient  $\alpha(B)$  of the paraexciton; dashed line, expected  $B^2$  dependence. Left inset:  $B$ -field dependence of energy shift  $\Delta E$ ; full dots, experimental results; solid line, fit to Eq. (1).

scattering rate at high field strength due to a low population of LA phonons. In the left inset we show the shift  $\Delta E$  of the paraexciton resonance as function of  $B$  field. The solid line shows the dependence expected from Eq. (1) with the parameters cited.

In Fig. 2 we present our two-phonon excitation spectrum taken in Faraday configuration ( $\mathbf{B} \parallel \mathbf{k} \parallel [110]$ ) in a magnetic field of 10 T at  $T = 1.2$  K. The signal (quadrupole emission of paraexciton) is measured as function of laser energy  $E_L = E_P + E_{LO} + E$ , where  $E_P$  and  $E_{LO}$  are the paraexciton and  $\Gamma_5^-$  optical phonon energy values, respectively. Thus the laser energy  $E_L$  is at least by one LO-phonon energy  $E_{LO}$  above the paraexciton resonance  $E_P$ . For  $0 < E < E_1$  excitons are excited via a  $\Gamma_5^-$  phonon emission and are monitored after relaxation by quadrupole emission of the paraexciton. As shown in the inset, at  $E = E_1$  the emission of an additional longitudinal acoustic phonon sets in which prevails up to  $E = E_2$  and thus leads to the enhanced quadrupole emission. For the fit of the background we assume a square-root dependence as expected from the phonon-assisted absorption [17].

The resonance at  $E = 0$  is broadened because of the finite lifetime of the phonon. It is fitted by a Lorentzian (FWHM 4.5  $\mu\text{eV}$ ). From the reading of the high precision wave meter of the paraexciton resonance  $E_P$  and the laser reading at the phonon-assisted resonance ( $E_P + E_{LO}$ ), we get a very accurate value for the phonon energy  $E_{LO} = (10.58 \pm 0.01)$  meV. For the analysis of the kinematics it is advantageous to shift the axes origin to the resonance on the exciton parabola ( $nk_0, E_0$ ) and then derive expressions

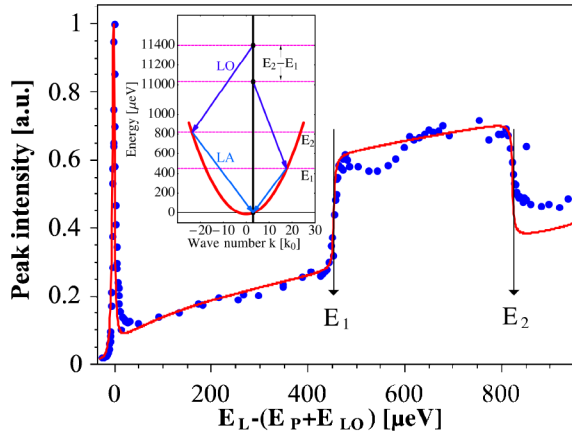


FIG. 2 (color online). Two-phonon excitation spectrum at 1.2 K monitored as quadrupole emission of paraexciton at  $E_P = 2.020598$  eV.  $E = 0$  corresponds to a laser energy  $E_L = E_P + E_{LO} = 2.031178$  eV. Full dots, experimental points; solid line is a fit to a Lorentzian (FWHM =  $4.5 \mu\text{eV}$ ) for the LO-phonon resonant process, a square-root dependent background and a plateau for the region of LO- and LA-phonon processes. Inset: schematics of the LO- and LA-phonon scattering. Zero energy corresponds to the energy at wave number  $nk_0$ , which is shifted from the minimum of the exciton parabola ( $k = 0$ ) by the kinetic energy  $E_0$ .

for  $M_P$ ,  $n$ , and  $E_0$  with the known slope  $v_{LA}$  of the phonon dispersion as function of  $E_1$  and  $E_2$ :

$$M_P = \frac{1}{4m_0c^2} \left( \frac{c}{v_{LA}} \right)^2 (E_2 + E_1), \quad (3)$$

$$n = \frac{1}{4E_P} \left( \frac{c}{v_{LA}} \right) (E_2 - E_1), \quad E_0 = \frac{1}{8} \frac{(E_2 - E_1)^2}{(E_2 + E_1)}.$$

From the fit of the rise and fall of the LA-phonon plateau in Fig. 2, we obtain  $E_1 = (453 \pm 3) \mu\text{eV}$  and  $E_2 = (820 \pm 3) \mu\text{eV}$ . For the velocity of sound we used  $v_{LA} = 4.63 \times 10^3 \text{ ms}^{-1}$ . This value is calculated from the room temperature measurements ( $v_{LA} = 4.56 \times 10^3 \text{ ms}^{-1}$  from Ref. [18]) by taking into account the temperature dependence of the elastic constants [19]. From Eq. (3) we derive the following values:  $M_P = 2.61 \pm 0.04$ ,  $n = 2.94 \pm 0.05$ , and  $E_0 = (13.2 \pm 0.2) \mu\text{eV}$ . The errors are calculated with the above errors of  $E_1$ ,  $E_2$  and a 1% error of  $v_{LA}$ . It should be noted that our method allows to determine  $E_0$  and thus  $n^2/M_P$  solely from  $E_1$  and  $E_2$ . With an independent measurement of  $n$  one can thus determine  $M_P$  without knowledge of  $v_{LA}$  and therefore even measure  $v_{LA}$ .

For the resonance absorption we observe with increasing excitation intensity an increase of the linewidth and in addition a blueshift of the absorption peak. The observation of a blueshift is especially important as it clearly indicates a repulsive exciton-exciton interaction potential. Assuming that the exciton-exciton scattering contributes additively to the exciton damping, we plot in Fig. 3 the difference of linewidth  $\hbar\Delta\Gamma$  at intensity  $I$  and lowest

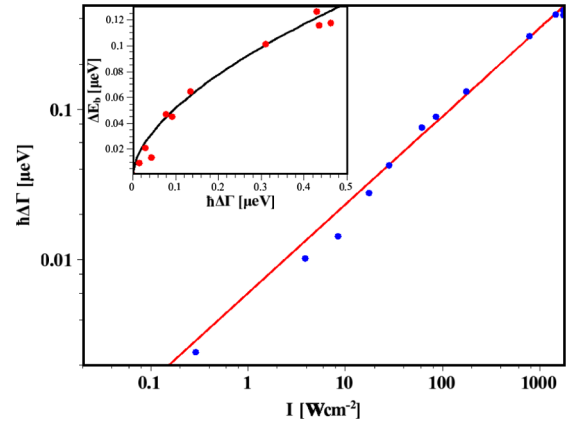


FIG. 3 (color online). Intensity induced line broadening  $\hbar\Delta\Gamma$  as a function of excitation intensity  $I$ ; solid line,  $\hbar\Delta\Gamma \propto I^{0.6}$ . Inset: intensity induced blueshift  $\Delta E_b$  as function of line broadening; full dots, experimental results; solid line,  $\Delta E_b \propto \hbar\Delta\Gamma^{0.6}$ .

intensity. A fit by a simple power law yields  $\Delta\Gamma \propto I^{0.6}$  (solid line). Assuming merely collision-induced broadening [5,20] as a mechanism for the increase of linewidth, we expect a linear dependence of  $\Delta\Gamma$  on the exciton density  $n_{\text{ex}}$

$$\Delta\Gamma = n_{\text{ex}} \sigma \bar{v}, \quad (4)$$

where  $\bar{v}$  is the average exciton velocity and  $\sigma$  the collisional cross section. The observed power dependence implies that the density increases only sublinear with excitation intensity, which is well known from many experiments on orthoexcitons [8] and explained by a bimolecular decay mechanism. The linewidth increases with laser intensity and thus the absorption coefficient  $\alpha$  decreases. For an intensity  $I = 1 \text{ kW/cm}^2$   $\alpha$  drops to  $15 \text{ cm}^{-1}$ . If one assumes that each photon missing in the detection channel leads to a paraexciton with lifetime  $\tau$ , one can estimate the paraexciton density  $n_{\text{ex}}$  [21]:

$$n_{\text{ex}} = \frac{I\alpha\tau}{\hbar\omega}, \quad (5)$$

where  $\hbar\omega$  is the energy of the incoming light.

The lifetime of the excitons under these excitation conditions is  $\tau = 150 \text{ ns}$ . With these parameters we obtain a density  $n_{\text{ex}} = 7 \times 10^{15} \text{ cm}^{-3}$ , which for an ideal Bose gas corresponds to a critical temperature of 0.4 K, a temperature which might be accessible by a  $^3\text{He}$  cryostat. The cross section for elastic scattering of excitons  $\sigma = 8\pi a_s^2$ , with  $a_s$  denoting the scattering length, has been calculated recently by a quantum Monte Carlo technique [22] for mass ratio of 1 (which almost applies to  $\text{Cu}_2\text{O}$ ). Their calculation yields  $a_s = 1.51a_B$  ( $a_B$  denoting the exciton Bohr radius) for antisymmetric scattering. Because of the spin alignment of the exciton states at high magnetic fields, the repulsive interaction does not contradict the recently proposed existence of a biexciton [8]. With  $a_B = 0.8 \text{ nm}$  [23] and the above estimate for the density, the broadening at

$T = 1.2$  K is  $0.3 \mu\text{eV}$ . This number has the right order of magnitude but it can only be taken as an estimate, since the effect of electron-hole exchange interaction was neglected in Ref. [22]. However, exchange interaction is known to influence strongly the exciton-exciton interaction potential [24].

As the shift of the exciton line results from the same physical mechanism of exciton-exciton interaction, we plot the dependence of the blueshift  $\Delta E_b$  on the line broadening as an inset in Fig. 3, which is a presentation independent of the exciton density. In contrast to the simple linear dependence expected from a hard core interaction [25], we again observe a sublinear dependence showing that a more rigorous analysis is needed that includes exciton diffusion and two-body decay. There is, however, a difficulty to get reliable values for the exciton density. As was recently discussed in Ref. [23], Lyman spectroscopy is a promising method to determine absolute densities of para- and orthoexcitons.

The results of high resolution spectroscopy of the paraexciton absorption are very promising for further experiments on excitation of high densities of ultracold paraexcitons towards BEC. Despite the fact that the oscillator strength of the paraexciton in a magnetic field of 10 T is only 0.006 of the oscillator strength of the quadrupole allowed orthoexciton, we achieved in carefully prepared and strain-free mounted samples an absorption coefficient up to  $80 \text{ cm}^{-1}$  and a linewidth of 80 neV. With our new method of two-phonon excitation spectroscopy we get reliable values of the paraexciton mass, which solves a long lasting discussion [10]. The importance of central cell corrections as discussed in Ref. [26] is thus confirmed. The higher background refractive index of 2.94 as compared to 2.55 [4,9,13] will lead to detailed corrections of the polariton dispersion and the anisotropic orthoexciton mass values [4,27]. The main advantage of our method lies in the fact that it provides reliable values of the exciton mass by a merely kinematical analysis, the accuracy of which is determined by the accuracy of the laser energy and the sound velocity. Line broadening and a blueshift at higher excitation intensity are caused by a repulsive exciton-exciton interaction, which is a prerequisite for a stable BEC.

We acknowledge the support by the Deutsche Forschungsgemeinschaft (SFB “Starke Korrelationen im Strahlungsfeld”, Graduiertenkolleg “Materialeigenschaften und Konzepte für die Quanteninformationsverarbeitung”, and Forschergruppe “Quantenoptik in Halbleitern”) and by the Japan Society for the Promotion of Science (Japan-Germany Research Cooperative Program “Macroscopic Quantum Phenomena in Electron-Hole Ensemble and Excitons”). We thank Makoto Kuwata-Gonokami and André Mysyrowicz for stimulating discussions.

- [1] D. Snoke, *Science* **298**, 1368 (2002).
- [2] J. Kasprzak *et al.*, *Nature (London)* **443**, 409 (2006).
- [3] R. Balili, V. Hartwell, D. Snoke, L. Pfeiffer, and K. West, *Science* **316**, 1007 (2007).
- [4] G. Dasbach, D. Fröhlich, H. Stolz, R. Klieber, D. Suter, and M. Bayer, *Phys. Rev. Lett.* **91**, 107401 (2003); *Phys. Rev. B* **70**, 045206 (2004).
- [5] J.P. Wolfe, J.L. Lin, and D.W. Snoke, *Bose-Einstein Condensation*, edited by A. Griffin, D.W. Snoke, and S. Stringari (Cambridge University Press, Cambridge, England, 1995).
- [6] T. Goto, M. Y. Shen, S. Koyama, and T. Yokouchi, *Phys. Rev. B* **55**, 7609 (1997).
- [7] M. Y. Shen, T. Yokouchi, S. Koyama, and T. Goto, *Phys. Rev. B* **56**, 13 066 (1997).
- [8] J.I. Jang and J.P. Wolfe, *Phys. Rev. B* **74**, 045211 (2006).
- [9] D. Fröhlich, G. Dasbach, G. Baldassarri Höger von Högersthal, M. Bayer, R. Klieber, D. Suter, and H. Stolz, *Solid State Commun.* **134**, 139 (2005).
- [10] M. Jörger, T. Fleck, C. Klingshirn, and R. von Baltz, *Phys. Rev. B* **71**, 235210 (2005).
- [11] *Handbook of Optical Constants of Solids II*, edited by E.D. Palik (Academic, New York, 1991), p. 875; B. Karlsson, C.G. Ribbing, A. Roos, E. Valkonen, and T. Karlsson, *Phys. Scr.* **25**, 826 (1982).
- [12] R. Schwartz and H. Stolz (to be published).
- [13] D. Fröhlich, J. Brandt, C. Sandfort, M. Bayer, and H. Stolz, *Phys. Status Solidi B* **243**, 2367 (2006).
- [14] G. Baldassarri Höger von Högersthal, D. Fröhlich, M. Kulka, T. Auer, M. Bayer, and H. Stolz, *Phys. Rev. B* **73**, 035202 (2006).
- [15] G. Kuwabara, M. Tanaka, and H. Fukutani, *Solid State Commun.* **21**, 599 (1977).
- [16] D. Fröhlich and R. Kenkies, *Phys. Status Solidi B* **111**, 247 (1982).
- [17] P.D. Bloch and C. Schwab, *Phys. Rev. Lett.* **41**, 514 (1978).
- [18] J. Berger, *Solid State Commun.* **26**, 403 (1978).
- [19] J. Hallberg and R.C. Hanson, *Phys. Status Solidi* **42**, 305 (1970).
- [20] D.W. Snoke, D. Braun, and M. Cardona, *Phys. Rev. B* **44**, 2991 (1991).
- [21] J.M. Blatt, K.W. Böer, and W. Brandt, *Phys. Rev.* **126**, 1691 (1962).
- [22] J. Shumway and D.M. Ceperley, *Phys. Rev. B* **63**, 165209 (2001).
- [23] T. Tayagaki, A. Mysyrowicz, and M. Kuwata-Gonokami, *J. Phys. Soc. Jpn.* **74**, 1423 (2005).
- [24] F. Bassani and M. Rovere, *Solid State Commun.* **19**, 887 (1976).
- [25] H. Shi, G. Verechaka, and A. Griffin, *Phys. Rev. B* **50**, 1119 (1994).
- [26] G.M. Kavoulakis, Y.-C. Chang, and G. Baym, *Phys. Rev. B* **55**, 7593 (1997).
- [27] G. Dasbach, D. Fröhlich, H. Stolz, R. Klieber, D. Suter, and M. Bayer, *Phys. Status Solidi C* **2**, 886 (2005).